Removal of chromium(VI) from wastewater via polyvinyl alcohol and polyvinyl alcohol/chitosan encapsulated onto Jojoba leaves: fixed-bed column studies

Amina A. Attia*, Mona A. Shouman, Soheir A. Khedr, Gehan A. Fagal

*Department of Physical Chemistry, National Research Center, 12622 El-Behouth St., El-Dokki, Giza, Egypt, Tel. +202 33371-433;
Fax: +202 33370597; emails: amina_abdelmeguid@yahoo.com (A.A. Attia), monashouman@yahoo.com (M.A. Shouman),
soheir.atty@yahoo.com (S.A. Khedr), gehanfagal@gmail.com (G.A. Fagal)*

ABSTRACT

Exhaustive industrial and urban development aroused the release of environmental pollutants. Cr(VI) is one of the most toxic and adequate prevalent throughout the heavy metal pollutants of industrial wastes. The present work directed towards the ability of raw Jojoba leaves treated with PVA (RJP) and a binary polymeric blend of PVA/chitosan (RJPC) as a novel adsorbent for the recovery of Cr(VI) ions from aqueous solutions employing fixed-bed column studies. Vital design parameters such as flow rate, bed depth and impact of pH were performed were performed. Characterization of the samples was conducted using a scanning electron microscope, Fourier transform infrared spectroscopy and energy dispersive X-ray spectroscopy analysis. Data analysis revealed that by increasing the bed height (4 cm) and decreasing flow rate (4 ml/min); the breakthrough and exhaustion time favorably increased. Moreover, Adams–Bohart modal utilized the experimental analysis to predict column performance. However, the bed depth service time model was applied to signify the impact of bed depth on breakthrough curves. Regeneration studies were successfully repeated in three cycles with 0.1 N HCl eluant and PVA/Chitosan validates its efficacy as a low-cost adsorbent for the recovery of Cr(VI) from aqueous solution.

Keywords: Adsorption; Chromium(VI); Fixed-bed column; Jojoba leaves; Modeling

1. Introduction

The rigorous evolution of metallic contaminants in aquatic system arising from various industrial epoch is presently one of the greatest essential environmental subjects being analyzed [1]. The leakage of heavy metals within the environment alters the human being health, aquatic life and the thorough ecosystem owing to their complex nature of existence and non-biodegradability [2]. Even at lower concentrations, heavy metals can assimilate inside the living tissues of an organism causing diverse effects [3]. Hexavalent chromium has extensively participated in many industries like (Steel and nonferrous alloy) as metallurgical industries, leather tanning, paint and pigments refractory's (chromate- magnetite and chrome), electroplating, timber treatment [4,5]. World Health Organization [6] appoints the maximum limit for Cr(VI) recommended by US EPA as 0.1 mg/L for release into domestic surface water, and 0.05 mg/L in freshwater. Hexavalent chromium is highly toxic due to the negatively charged Cr(VI) ion complexes that go throughout the cellular membranes through sulfate ionic channels and then go through direct reduction reactions leading to the elaboration of a diverse harmful reactive intermediary. Since its salts are soluble, causing its high mobility and thus can be efficiently absorbed and accumulated in the human body causing lung tumors, severe diarrhea, skin irritation, internal hemorrhage and respiratory problems [7,8]. Since Cr(VI) causes a great threat to

* Corresponding author.

the environment ecosystem, cleaning up this contaminant from soil and water is vital. The major processes that could be applied for the removal of Cr(VI) are reduction followed by chemical precipitation [9]. Other techniques such as electrokinetic remediation, biosorption and membrane separation processes are being applied to discharge Cr(VI) [10]. The disadvantage of using these methods is the consumption of chemical agents and the production of huge amounts of sludge.

Currently, the most common technique for eliminating Cr(VI) is adsorption. In order to transfer the adsorption technique of Cr(VI) from scaling laboratory to pilot scale, it is crucial to perform the experiments in a fixed bed column. This technique possesses numerous advantages such as; little operator attention, simple inspection, cleaning for the regeneration of the adsorbent and minor instances of adsorbent particles in the effluent [11]. The achievement of packed beds has been outlined through the concept of breakthrough curves.

The employment of low-cost adsorbents and biomaterials (by-products or agricultural wastes materials from huge-scale industrial operations) have received a great deal of attention the past years as a result of the well-known functional groups present such as pectin, lignin, and cellulose which can easily promote the binding of heavy metals [12]. Jojoba plants (*Simmondsia chinensis*) are generally cultivated in the southern area of Egypt; its seed wax is used in cosmetic manufacturing and as a lubricant with noticeable performance in a wide region. Jojoba leaves have stated as an innovative adsorbent for the elimination of heavy metals from aqueous solutions [13]. Surface modification was achieved by adding the polymer to the adsorbent. Polymeric substances are promising as an adsorbent composite as a result of their good mechanical rigidity, alterable surface chemistry [14] in addition to their good selectivity toward inorganic and organic adsorbate [15]. Nevertheless, their efficiency is dependent on the type of functional groups used, that is, type and degree of functionality grafted on the polymeric surface. Polyvinyl alcohol (PVA) is a water-soluble polymer with biocompatibility, biodegradability and non-toxicity nature [16]. Another decisive factor affecting the suitability of PVA is its hydrophilicity due to the regular linear structure accompanied by a great number of hydroxyls on the sides of the molecular chain.

Natural polysaccharide chitosan, a derivative of chitin [17] is of considerable concern as an organic compound in the composites developed for water remediation owing to the presence of amino and hydroxyl groups, which is crucial for sorption processes [18]. Additionally, chitosan has high adhesion to the surface, a wide range of pH stability and signified as a chelating agent. It has been validated that chitosan is an efficient biosorbent towards inorganic and organic contaminants. Chitosan blended with polyvinyl alcohol has been noted to have good mechanical and chemical properties and has been appealed for the removal of heavy metals from aqueous solution [19].

One of the main disadvantages of adsorption is the pollution generated by the dumping of the spent adsorbent. To conquer this drawback, regeneration methods have been applied to re-establish the utmost adsorbent capacity and retain, as much as possible, the initial weight and pore structure of the adsorbent. Chemical regeneration of the adsorbent is a beneficial technique, it could be operated in situ, in which there is no damage to the adsorbent, feasible to improve valuable adsorbate and the chemical reagents could be recycled [20].

As a continuation of our previous works [21], the present research reports the possibility of raw Jojoba leaves to be blended with PVA in addition to PVA/Chitosan to uptake Cr(VI) ions from aqueous solutions in column study. The effect of some operating parameters such as flow rate, bed height and pH were considered. The shape of the breakthrough curve has been examined to compare the solid-phase loading and exhaustion time on the fixed bed. Two well-established fixed-bed adsorption models designed the dynamic of the adsorption process: Adams–Bohart and bed depth service time model (BDST) models. Column regeneration has been directed through three cycles to confirm the practical applicability of the investigated adsorbents for great scale industrial applications.

2. Materials and methods

2.1. Reagents

Polyvinyl alcohol applied in this study was of analytical grade and purchased from Fisher Chemicals (UK). The average Mw of PVA was 25,000 g/mol and the degree of hydrolysis is 88%. Chitosan (Mw = 600.000–800.000 g/mol) from ACROS OREAMCS, USA. Acetone, acetic acid, hydrochloric acid and sulfuric acid were obtained from Merck Company (Darmstadt, Germany) and applied without further purification.

2.2. Analysis of adsorbate stock solution

A stock solution of Cr(VI) was prepared by dissolving 2.83 g of $K_2Cr_2O_7$ in a 1,000 mL volumetric flask by dilution with double deionized water. Sample solutions of lower concentrations were prepared by appropriate dilution. The initial pH of the solution was adjusted by the addition of dilute HCl or NaOH utilized with a pH meter. The concentration of residual Cr(VI) ions in the effluent were recorded spectrophotometrically by using 1,5 diphenyl carbazide as the complexing agent under the controlled acidic conditions at pH = 2. The color of the complex solution progressively developed into pink-violet until it becomes stable within 30 min. Moreover, the solution absorbance was recorded at 540 nm [22].

2.3. Preparation of adsorbent

Jojoba leaves biomass was gathered from southern Egyptian deserts and washed thoroughly with hot water followed by rinsing with deionized – distilled water to remove from dirt and dust, then dried at 60°C for overnight. The dried Jojoba leaves were cut, grinded and passed through a 4 mm molecular sieve and stored in a desiccator. The sample was nominated as RJ.

2.4. Surface modification of Jojoba leaves

Surface modification was performed by dissolving 6 g PVA in deionized – distilled water and heated at 90°C with

constant stirring for 5 h. Afterward, Jojoba leaves (12 g) were immersed into this solution for another 2 h followed by sonification. This sample was nominated as RJP.

An accurately weighed 10 g chitosan flakes were dissolved in 10% (*w/v*) glacial acetic acid solution with continuous stirring for 4 h to obtain a white gel. Meanwhile, PVA (10g) was dissolved in 100 cm³ distilled water under constant stirring at 90°C for 4 h. The two previous solutions were blended together based on the desired mass ratio (50:50). Later, Jojoba leaves (12 g) were added to the solution which was then subjected to continuous mechanical stirring at 3,000 rpm for 1 h until a homogeneous suspension is obtained followed by sonification for 20 min. This sample was abbreviated as RJPC.

2.5. Characterization of samples

The surface and matrix morphology of the investigated samples were observed on a JEOL Model JSM, 5,300 LV, scanning electron microscope (SEM). Quantitative analysis of elemental composition was examined by energy-dispersive X-ray spectroscopy (EDX). The samples were recorded by utilizing a transform infra-red spectrophotometer (Perkin Elmer FTIR 2000). IR spectra were scanned over the spectral range of 4,000–400 cm⁻¹.

2.6. Fixed-bed column setup and operations

A fixed-bed column is extensively used as an effective process for adsorption–desorption studies [23]. The proficiency of a fixed-bed column is demonstrated through the concept of the breakthrough curve. The shape of this curve, as well as, the time required for breakthroughs are essential for determining the operation and dynamic response of an adsorption column. Sorption studies were conducted in a laboratory-scale glass column with an internal diameter of 2 and 50 cm in length. All experiments were conducted at room temperature. The column was packed with the different investigated samples separately fitted between two supporting layers of quartz sand to guarantee the proper distribution of the inlet solution. The adsorbents were added from the top of the column and permitted to settle down by gravitation. Before the beginning of column experiments, the beds were flushed out with distilled water and kept overnight to establish a compactly packed arrangement of particles with no voids, cracks, or channels. Cr(VI) solution was supplied through the column in a downflow mode by using a peristaltic pump (Rivotek) TM. The samples of the effluent solution were gathered at a specific time interval, and the concentration of the output solution was measured using a UV-Vis spectrophotometer. The effect of inlet flow rate (4 and 6 ml), bed height (1, 2.5, and 4 cm) and influent pH (2, 6, and 8) were percolated to determine the column breakthrough performance.

2.7. Data analysis

In fixed-bed studies, the adsorption efficiency of column studies is described through the concept of a breakthrough curve (BC). Mainly, breakthrough curves demonstrate characteristics *S*-shape with different degrees of position and steepness of the breakthrough point. The breakthrough curve is generally expressed by C_t/C_0 as a function of time or volume of the effluent for a definite bed height with varying operating conditions. The breakthrough point (C_b) is reached when the effluent concentration reaches up to 5% of its initial value, while the point of column exhaustion (C_e) is considered the point where the effluent concentration reaches 95% of its initial concentration. The overall sorption zone (Δt) was evaluated by applying the following equation [24]:

$$\Delta t = t_e - t_b \tag{1}$$

where t_e and t_b are the breakthrough time (at 50%) and exhaustion time (at 99%) of effluent concentration, respectively.

In addition, the effluent volume (V_{eff}) can be obtained from the following equation [24]:

$$V_{eff} = F \times t_{total} \tag{2}$$

where F is the flow rate (ml/min) and t_{total} is the total flow time (min).

The influent Cr(VI) concentration in a fixed-bed column creates a wavefront through the adsorbent bed known as the mass transfer zone (Z_m) or also termed as critical bed length, which is related to bed height, breakthrough and exhaustion time. Mass transfer begins instantly upon the introduction of influent, leading to a decrease in adsorbate concentration throughout the length of the bed until it reaches nearly zero. It can be determined by using the following equation [24]:

$$Z_m = Z\left(1 - \frac{t_b}{t_e}\right) \tag{3}$$

where Z is the bed height (cm)

The resin exhaustion rate (RER) is identified as the mass of resin used per volume of liquid treated at breakthrough [25]

$$RER = \frac{\text{Mass of resin in fixed-bed column}}{\text{volume treated at break through}} \tag{4}$$

Industrially, a bed is operated until the effluent reaches breakpoint concentration. At this point, the bed is not fully exploited for effluent uptake. Therefore, a term named LUB which is defined as the equivalent length of unused bed can be evaluated by the following equation [25]:

$$LUB = \frac{Z}{t_e}(t_e - t_b) \tag{5}$$

The empty bed contact time (EBCT) is a vital parameter in fixed-bed adsorption column study. It is defined, as the time needed for the liquid to fill the empty column. It is calculated by using the following equation [26]

$$EBCT = \frac{\text{Bed Volume}}{\text{Flow rate}} \tag{6}$$

where bed volume = bed height X cross-sectional area of the column.

2.8. Modeling of column data

In recent years, simple mathematical models can signify the succeeding operation of a lab-scale column through industrial applications. In the present study, two well-known mathematical models, namely, the BDST and Adam–Bohart's model, anticipated the breakthrough curves attained for bed height, flow rate and pH.

2.8.1. Adams–Bohart's model

Adams–Bohart model is often applied for representing a fixed-bed column breakthrough at the initial state of the operation. This model presumes that the adsorption rate is proportional to the fraction of adsorption capacity that remains on the surface of the adsorbent. The mathematical equation can be expressed as following [27]:

$$\ln = \left(\frac{C_t}{C_0}\right) = K_{AB}C_0 t - K_{AB}N_0\frac{Z}{F} \tag{7}$$

where C_0 and C_t are the inlet and outlet adsorbate concentrations (mg/L), K_{AB} is the mass transfer coefficient (L/mg min), t is the time (min), N_0 is the saturation concentration (mg/L), Z is the bed depth of the column (cm) and F is the superficial velocity of the influent concentration and defined as the ratio of the volumetric flow rate (Q, cm³/min) to the cross-sectional area of the bed (A, cm²). The parameters describing the characteristic operations of the column (K_{AB} and N_0) were calculated from the intercept and slope of the linear plot of $\ln(C_t/C_0)$ vs. time (t), respectively. [Figure not shown]

2.8.2. BDST model

The BDST model proposed from the model described by Bohart and Adams was applied to express the relationship between column bed depth (Z) and service time (t) at breakthrough. It estimates that the rate of adsorption is governed by the surface reaction between the adsorbate and the unspent capacity of the adsorbent. It doesn't consider the intraparticle mass transfer resistance, besides the external film resistivity where the adsorbate is directly adsorbed onto the surface of the adsorbent. The linear form of the BDST model can be expressed by the following equation [28]:

$$t = \frac{N_0 Z}{C_0 F} = \frac{1}{K_a C_0}\ln\left(\frac{C_0}{C_t}-1\right) \tag{8}$$

where N_0 is the dynamic capacity (mg/L), Z is the bed height (cm), C_0 and C_t are the influent and effluent Cr(VI) concentration (mg/L), F is the linear flow rate of solution (cm/min), t is the service time (min), and K_a is the adsorption rate constant that explains the mass transfer from the liquid phase to solid phase (L/mg min). Thus, N_0 and K_a can be accessed from the slope and intercept of the plot of t vs. bed depth (Z), accordingly. The rate constant, K_a is a measure of the rate transfer of Cr(VI) solution from the liquid phase to solid phase.

2.9. Column regeneration study

Recycling of adsorbent has an important significance for the application of column study from laboratory to industrial scale. In this research, regeneration of adsorbent was performed using 0.1 N HCl solution through the bed in a downward direction with a flow rate of 4 ml/min for 24 h through the column after every service cycle. This allows sufficient exchangeable H⁺ ions to desorb Cr(VI) ions completely. After each cycle, the bed was thoroughly washed with hot distilled water until the pH of the wash effluent stabilized to 7. The adsorbents were then dried at 50°C for 5 h and then packed inside the column for further regeneration studies. The regeneration efficiency was calculated for the bed height (4 cm) and initial concentration of 25 mg/L by applying the following equation [29]:

$$\text{Regenerated efficiency }(\%) = \frac{t_b(\text{regenerated bed})}{t_b(\text{fresh bed})} \tag{9}$$

3. Results and discussion

3.1. Characterization of adsorbents

3.1.1. SEM and EDX analysis

The morphology of the investigated samples and its EDX analysis are displayed in Figs. 1a–c. Fig. 1a represents RJ which shows a rough and non-homogenous topography with striated and shrank surface [30]. However, RJP indicates a random oriented porous structure as obvious from Fig. 1b. In addition, the image of RJPC illustrated that the chitosan, PVA, and JL have an excellent blend without any considerate aggregation. This blending has improved the porosity, which in turn facilitates the adsorption capacity of Cr(VI) (Fig. 1c).

EDX analysis depicted the elemental composition of these materials. It was observed that the main components of the investigated samples were mainly carbon and oxygen with different percentages. Along with this, blending with PVA led to an increase in the percentage of oxygen.

Furthermore, nitrogen, aluminum, silicon, were also, predicted in the EDX spectra presumably which originates from chitosan. This confirms that the mixing of chitosan with PVA was successful on the surface of jojoba [31] (Table 1).

3.1.2. Fourier transform infrared spectroscopy (FTIR) analysis

The investigated samples were assessed by FTIR spectra, as presented in Figs. 2a–c. Fig. 2a represents a broad and strong band at 3,316 cm⁻¹ which was attributed to –OH group of JL. The peaks at 2,923, 2,853, and 2,751 cm⁻¹ represent asymmetric and symmetric stretching vibration of –CH₂ groups [32,33]. The absorption band at 1,632 and 1,438 cm⁻¹ were assigned to –C=O and COO groups. While the peak at 1,520 cm⁻¹ refers to C=O stretching of the carboxylic group [34].

As revealed in Fig. 2b, PVA exhibited stretching vibration peak of its side hydroxyl group at 3,294 and 1,027 cm⁻¹. The absorption bands at 2,922; 2,853; and 1,438 cm⁻¹ were assigned to the stretching vibration and bending vibration
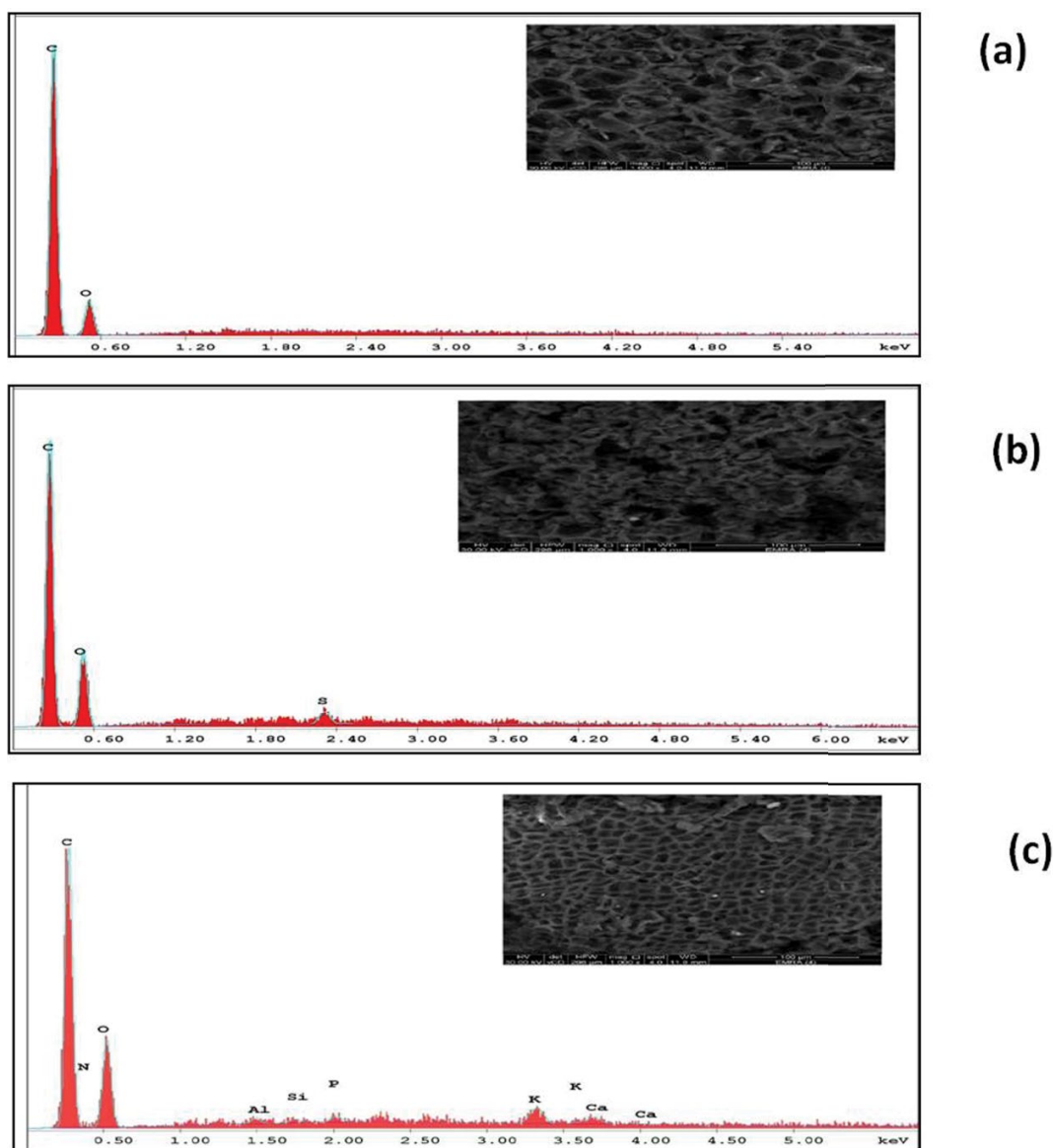
Fig. 1. SEM and EDX of (a) RJ, (b) RJP, and (c) RJPC.

Table 1
Elemental analysis of the investigated samples

	Elemental analysis		
Element	RJ	RJP	RJPC
C	74.8	64.4	56.81
O	25.2	34.7	35.74
S	–	0.88	–
N	–	–	4.57
Al	–	–	0.45
Si	–	–	0.28
P	–	–	0.40
K	–	–	1.18
Ca	–	–	0.58
Total	100	100	100

of –CH, respectively [35]. A significant peak is verified at 1,026 cm^{-1} that is mainly attributed to the crystallization of PVA, related to the carboxyl stretching group. Upon the addition of chitosan to PVA onto RJL, the intensity of the absorption peak at 3,365 cm^{-1} decreased indicating –OH and –NH stretch. This validated that the hydroxyl groups in the C-2 and C-6 positions of chitosan are combined by inter- and intramolecular hydrogen bonds between the amino and hydroxyl groups in chitosan, and PVA, respectively [36,37].

Characteristic peak at 1,636 cm^{-1} is ascribed to the C=N vibration of the imine group in addition to the bending vibration of the unreacted –NH group [36]. Another apparent feature was the appearance of new weak peaks at 2,211 and 1,962 cm^{-1}, which were assigned to the characteristic peaks of C=N stretching nitrile and –CH bending aromatic compound, respectively. The definite peak at 516 cm^{-1} corresponds to the saccharide structure of chitosan (Fig. 2c).
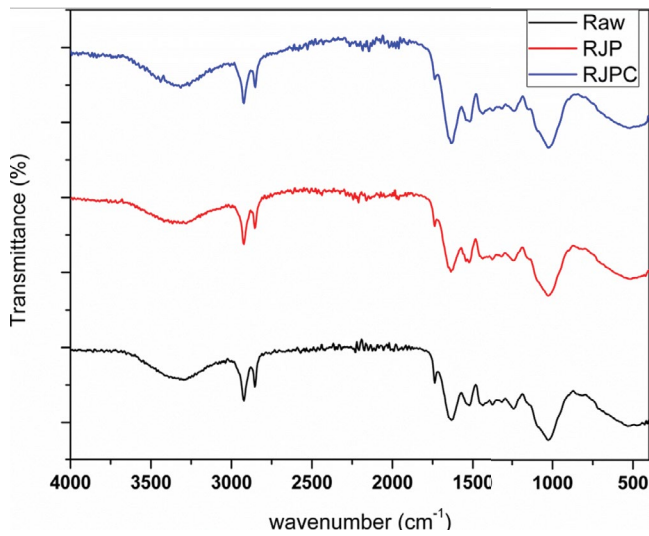
Fig. 2. FTIR of (a) raw, (b) RJP, and (c) RJPC.

Some common peaks in the range of 1,024–1,238 cm^{-1} were assigned for –CH groups. The shifting of these peaks may be taken as an indication of the involvement of PVA and Chitosan onto RJL.

Therefore, we propose that when polymers are blended, alteration in characteristic spectra peaks appear as a result of the change in physical and chemical interactions. These notifications display the existence of excellent miscibility of chitosan and PVA.

3.2. Optimization of column parameters

3.2.1. Effect of bed depth

The effect of bed depth on breakthrough experiments was conducted at 1, 2.5, and 4 cm using a constant flow rate of 4 ml/min and initial concentration of Cr(VI) (25 mg/L) at pH = 2. The breakthrough curves are displayed in Figs. 3a–c as well as the useful data obtained from these breakthrough curves are presented in Table 2. It can
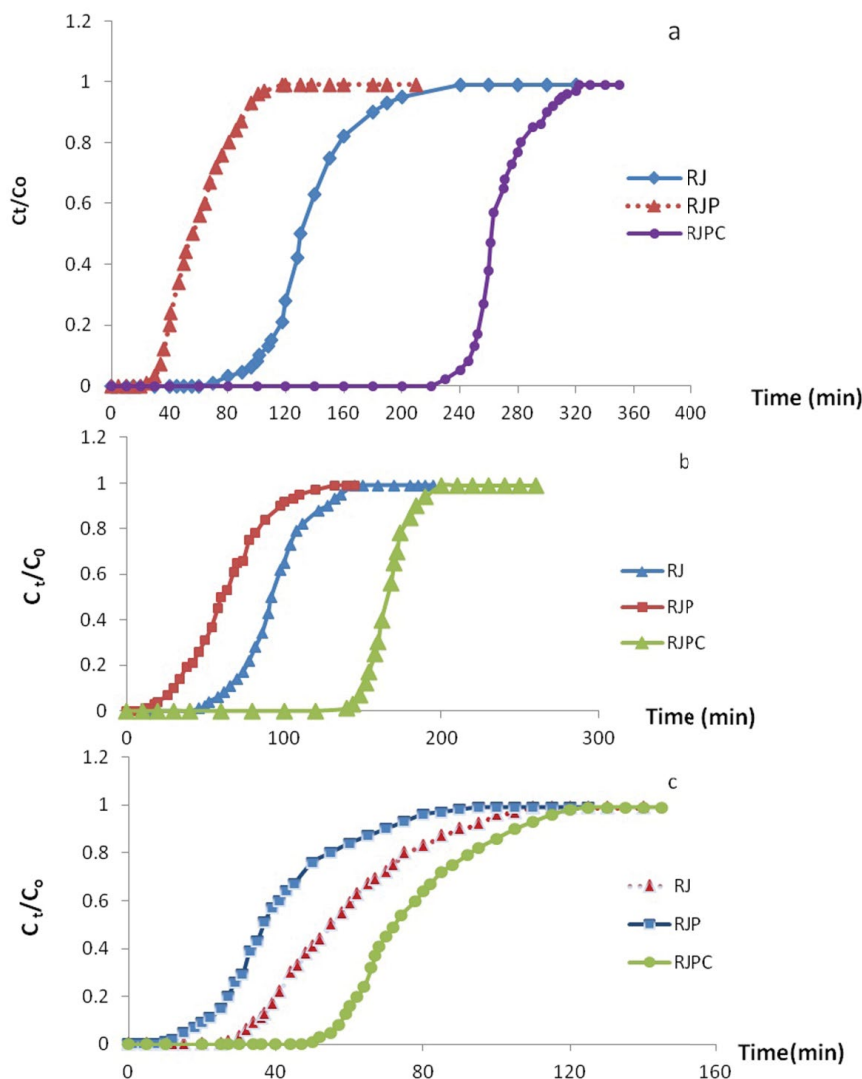
Fig. 3. Effect of different bed depth (a) 4 cm, (b) 2.5 cm, and (c) 1 cm at C_0 = 25 mg/L, flow rate = 4 ml/min and pH = 2.

Table 2
Parameters in fixed-bed column for Cr(VI) adsorption by RJ, RJP and RJPC

Sample	Flow rate (ml/min)	Bed depth (cm)	t_b at 0.05 (min)	t_e (min)	Z_m (cm)	RER (mg/ml)	LUB (cm)	EBCT (min)	BV	Δt (min)	V_{eff}
RJ	4	1	32	97	0.7	0.008	3.4	4	16	65	388
		2.5	60	135	1.4	0.01	3.6	5	20	75	540
		4	92	240	2.5	0.01	5	6	25	148	960
	6	4	40	105	2.5	0.02	4.9	4.2	25.1	65	630
RJPC	4	1	55	130	0.6	0.005	2.8	4	16	75	520
		2.5	147	210	0.8	0.004	2	5	20	63	840
		4	240	322	1.0	0.004	2	6	25	82	1,288
	6	4	60	130	2.2	0.01	4.3	4.2	25	70	780
RJP	4	1	15	78	0.8	0.02	4	4	16	63	312
		2.5	27	115	2.0	0.02	5	5	20	88	460
		4	32	140	3.0	0.03	6	6	25	108	560
	6	4	20	90	3.2	0.007	5.4	4.2	25	70	540

be identified that the increase in bed depth leads to longer breakthrough exhaustion time of adsorbents. This is owing to that at higher bed depth, the diffusion of Cr(VI) towards different adsorbents is controlled over the axial dispersion, which provides more surface area and adsorptive sites for adsorption [38]. The breakthrough cures became steeper by decreasing the bed depth, which in turn decreased the length of the mass transfer zone. The clear remark of Table 2 implies that breakthrough time, bed exhaustion time, overall adsorption zone and effluent volume increased by increasing the bed depth for all the investigated samples. Additionally, the mass transfer zone broadened whilst bed volume and empty bed contact time increased upon increasing the bed depth owing to the increase in the residential time of Cr(VI) inside the column bed. These results clarify that the most efficient adsorbent for Cr(VI) adsorption is RJPC.

3.2.2. Effect of flow rate

An essential parameter in analyzing the efficiency of an adsorption mechanism, particularly for the continuous treatment of wastewater in the industrial system is the flow rate. Therefore, the influence of flow rate on adsorption of Cr(VI) via the investigated samples was conducted by altering the flow rate from 4 to 6 ml/min while maintaining the initial Cr(VI) concentration and bed depth constant (25 mg/L and 4 cm, respectively). The breakthrough curves are presented in Figs. 4a and b, showing that breakthrough curves (BT) decreased with increasing the flow rate. Table 2 displays that with increasing flow rate, EBCT declined from 6.3 to 4.2 accompanied by a decrease in exhaustion time as a whole adsorption zone and the length of the mass transfer zone. This behavior could be ascribed as by increasing the flow rate, the residence time of Cr(VI) solution in the column decreases resulting in a deficiency in contact time between adsorbent and adsorbate. Thus, the surfaces of adsorbents don't have enough time to bind efficiently to the metal molecules of Cr(VI) leaving the column before equilibrium occurs [39].

3.2.3. Impact of influent pH

The pH adsorption process is a decisive constituent having an effect on the sorption of metal ions. The point of zero charge (pH_{pzc}) has a vital role in the ionic state of functional groups existing on the surface of adsorbents. If the pH is below or above the point of zero charge, the surface charge becomes positive and negative, respectively. In this study, the pH_{pzc} of RJ, RJP, and RJPC was found to be 4.0 ± 5.0. Below this pH value, the surface charge of the investigated samples was positive that associates a protonation of the functional groups which exist upon the adsorbent's surface. Furthermore, in acidic pH, the Cr(VI) ions exist in its possible oxyanions form like $HCrO_4^-$, CrO_4^- and $Cr_2O_7^{-2}$. The mechanism reaction in an acidic medium can be represented as follows:

$$HCr_2O_7 \rightarrow H^+ + Cr_2O_7^{-2} \tag{10}$$

$$HCrO_4 \rightarrow H^+ + Cr_2O_4^- \tag{11}$$

while in a basic medium is given as:

$$Cr_2O_7^{-2} + OH^- \rightarrow HCrO_4^- + CrO_4^{-2} \tag{12}$$

$$HCrO_4^- + OH^- \rightarrow CrO_4^{-2} + H_2O \tag{13}$$
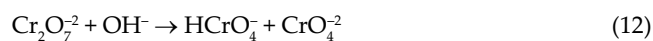
The impact of pH for the efficiency of the column was investigated in the pH range of 2,4 and 5 while maintaining flow rate, inlet Cr(VI) concentration and bed depth at constant values of 4 ml/min, 25 mg/L and 4 cm, respectively for RJPC sample. It is evident from Fig. 5 that breakthrough curves shifted from left to right associated with a reduction in pH yielded the longest breakpoint time. So, pH = 2 was selected as the optimal pH for our study. This can be ascribed that at pH = 2, the solution is acidic and contains amine and hydroxyl groups which belong to chitosan and PVA as confirmed from FTIR. These groups are easily protonated

A.A. Attia et al. / Desalination and Water Treatment 190 (2020) 203–214
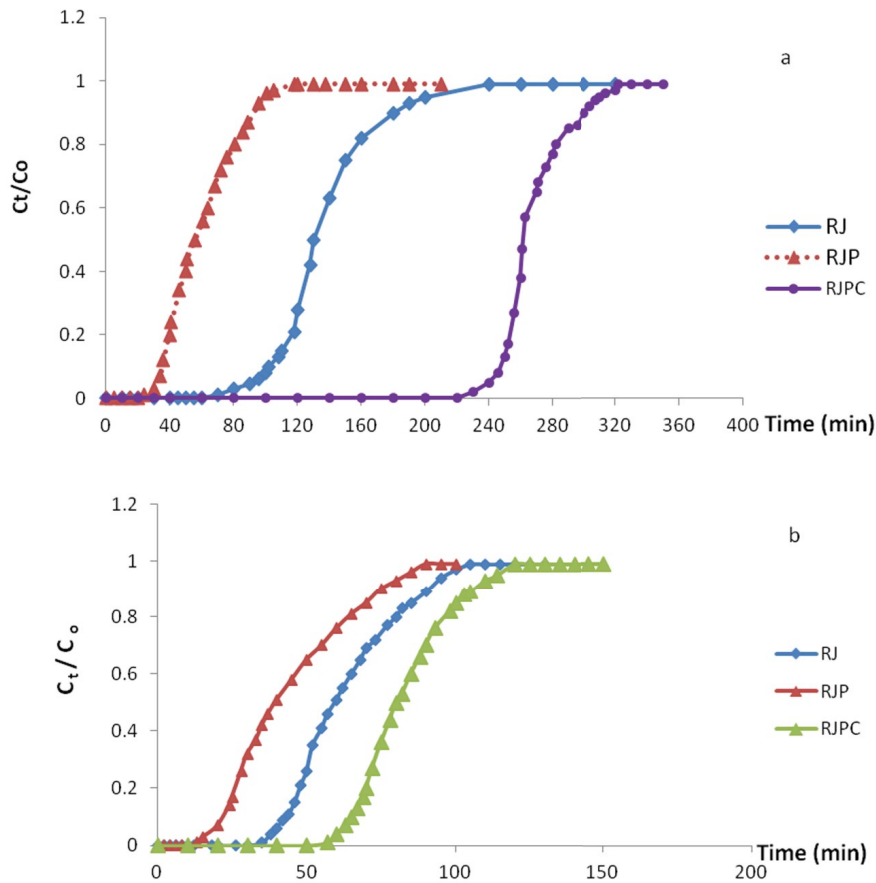
Fig. 4. Effect of different flow rate (a) 4 ml/min and (b) 6 ml/min at C_0 = 25 mg/L, bed depth 4 cm and pH = 2.
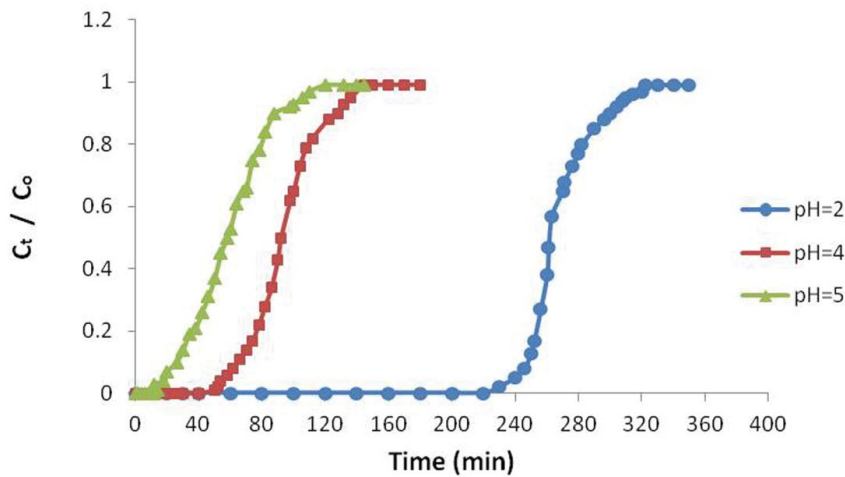
Fig. 5. Effect of pH on Cr(VI) removal by RJPC (C_0 = 25 mg/L, flow rate = 4 ml/min and bed depth = 4 cm).

to NH_3^+ and OH_2^+ which facilitate the electrostatic attraction toward the oxyanions Cr(VI) [37,38,40].

4. Modeling of experimental data

In order to illustrate the fixed bed column performance and arise for its industrial applications, two models namely Adam–Bohart, and BDST were used to relevant the column

behavior of adsorbent – adsorbate system from the experimental column data.

4.1. Adams–Bohart model

Adams–Bohart model covered the experimental data and explanation of the initial part of the breakthrough curve. This model emphasized on the evaluation of the characteristic

Table 3
Adam–Bohart parameters for column adsorption of Cr(VI) onto the investigated samples

Sample	C_0 (mg/L)	pH	Flow rate (mL)	Bed depth (cm)	K_{AB} (L/mg min)	$N_0 \times 10^{-3}$ (mg/L)
RJ	25	2	4	1	0.32	0.48
				2.5	0.34	0.19
				4	0.36	0.18
			6	4	0.27	170
RJPC	25	2	4	1	0.19	0.64
				2.5	0.25	0.74
				4	0.28	0.3
			6	4	0.34	110
RJP	25	2	4	1	0.26	0.63
				2.5	0.27	0.37
				4	0.3	0.46
			6	4	0.25	350

parameters such as maximum adsorption capacity (N_0) and kinetic constant (K_{AB}). The values of K_{AB} and N_0 were calculated for all breakthrough curves and were depicted in Table 3 along with their correlation coefficient (R^2). It was observed that the kinetic constant (mass transfer coefficient) increased by increasing the bed height, however, it decreased by increasing the flow rate [41,42]. While the sorption capacity (N_0) reduced slightly upon increasing the bed depth and increased by increasing the flow rate. This displayed that the overall system kinetics was governed by external mass transfer in the part of adsorption in column [43]. Despite that the Adams–Bohart model gives a simple and comprehensive way to manage and determine adsorption column tests, its efficacy was restricted to the range of conditions applied.

4.2. BDST model

The BDST model is governed by the Bohart and Adams quasi-chemical rate law. This model is predicated on the theory that the adsorption rate is sustained by the surface reaction between the unused capacity of the adsorbent and the adsorbate. It is established on physically measuring the capacity of the bed at various breakthrough values. Basically, this model avoids the intraparticle mass transfer and external film resistance. With these assumptions, the BDST model gives valuable modeling equations for the changes in the system parameters. Figs. 6a–c represents the bed height vs. service time at C_t/C_0 (0.2, 0.3 and 0.4) for the three adsorbents in a column with constant influent Cr(VI) concentration of 25 mg/L, a flow rate of 4 ml/min and pH = 2. The data were
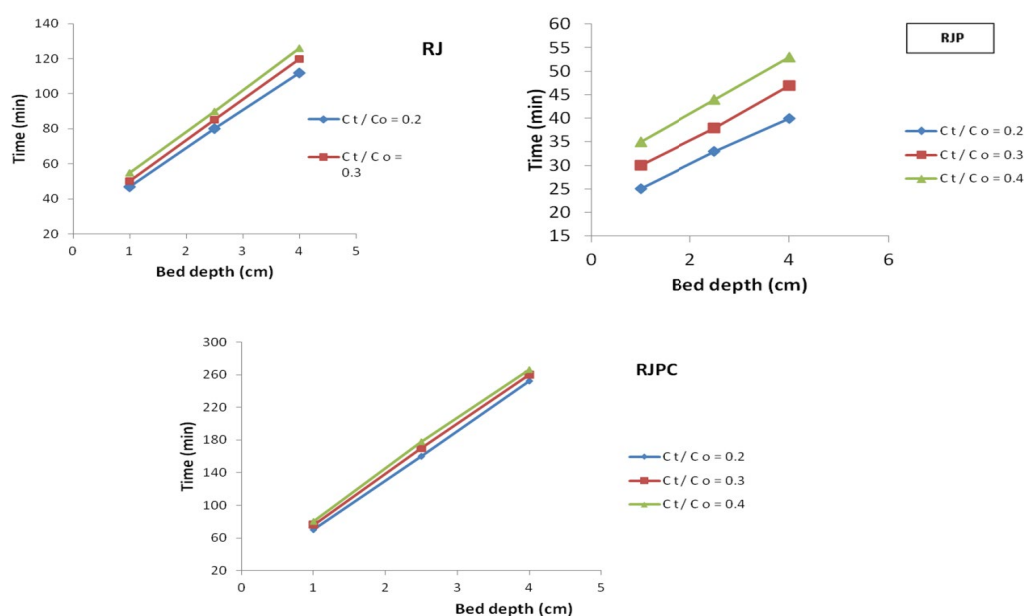
Fig. 6. BDST model plot for Cr(VI) adsorption onto the investigated samples.

attained with linear regression (R^2) between 0.97–0.99 displaying the suitability of the BDST model in representing the adsorption of Cr(VI) in the current study. As per assumption, the BDST data (K_a and N_0) are tabulated in Table 4 and the results indicated that the value of the constant K_a decreased whereas N_0 increased with increasing the ratio of C_t/C_0 for the

three investigated adsorbents. This could be ascribed to the significant increase in the number of available sites at higher bed heights. The obtained results are aligned by several researchers [44,45].

4.3. Column regeneration studies

The elute of heavy metals is essential for the reusability of exhausted adsorbents and the commercial validity of

Table 4
BDST parameters for column adsorption of Cr(VI) onto the investigated samples at $C_0 = 25$ mg/L and flow rate = 4ml/min

Sample	C_t/C_0	$K_a \times 10^{-3}$ (ml/mg min)	N_0 (mg/ml)
RJ	0.2	2.6	796
	0.3	1.5	892
	0.4	0.7	956
RJPC	0.2	0.92	319
	0.3	0.57	573
	0.4	0.27	764
RJP	0.2	10	637
	0.3	5	764
	0.4	2	892
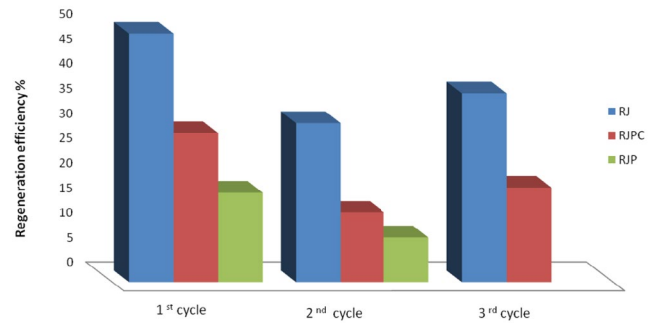
Fig. 7. Reuse of the investigated samples for Cr(VI) removal.
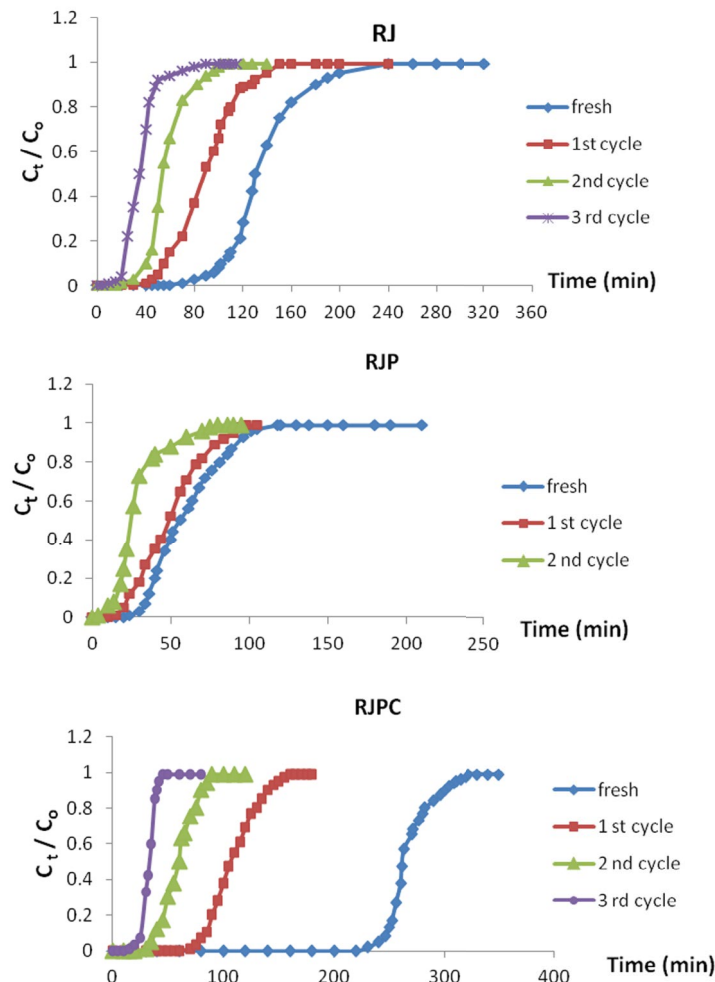
Fig. 8. Regeneration cycles of the investigated samples for Cr(VI) removal.

Table 5
Desorption process parameters obtained during each cycle for Cr(VI) using the investigated samples

Sample	Cycle No.	t_b at 0.05	t_b at 50%	t_e	RE (%)
RJ	Fresh	92	130	240	original
	1	46	88	120	50
	2	28	44	74	30
	3	17	32	44	18
RJPC	Fresh	240	262	322	original
	1	76	106	200	32
	2	33	60	85	14
	3	21	40	55	9
RJP	Fresh	32	56	140	original
	1	12	18	30	38
	2	6	10	15	19

the process. Therefore, attempts were done to regenerate and reuse the investigated samples over three cycles. The regeneration efficiencies were calculated using equation 8 (Fig. 7) and tabulated in Table 5.

Referring to Table 5 it was detected that the exhaustion time and regeneration efficiency decreased after each cycle as revealed in Fig. 8. This could be ascribed to the unacceptable effect of the acid eluent on the surface functional groups or binding sites. This demonstrates that the gradual deterioration of the column was affected by acid treatment. Additionally, this result is due to the continuous usage, and the available adsorption sites being blocked as a result of this process [46].

5. Conclusions

This work demonstrates that jojoba leaves either alone (JL) or being blended with polyvinyl alcohol (JLP) and mixed with polyvinyl alcohol and chitosan (JLPC) were tested as adsorbents for removing Cr(V1) from aqueous solution. The obtained investigated samples have been characterized by FTIR, SEM, and EDX. Fixed bed column studies were operated by changing the parameters, in particular, the flow rate, pH and bed depth. An increase in bed depth and low flow rate bring about an increase in the sorption performance of the column. Based on the analysis conducted in this study, it was detected that at pH 2 the surface charge of JLPC was positive which favored the Cr(VI) adsorption in its available $HCrO_4^-$ anions manifested on its surface. The prediction of breakthrough curves was gained by applying Adams–Bohart, and the BDST model. Regeneration of Cr(IV) onto the examined samples revealed that these adsorbents could effectively retain the sorption potential over up to four cycles.

References

[1] H. Patel, Fixed-bed column adsorption study: a comprehensive review, Appl. Water Sci., 9 (2019) 1–17.
[2] R. Rajeshkannan, M. Rajasimman, N. Rajamohan, Packed bed column studies for the removal of dyes using novel sorbent, Chem. Ind. Chem. Eng. Q., 19 (2013) 461–470.
[3] S. Sugashini, K.M. Meera, S. Begum, Column adsorption studies for the removal of Cr(VI) Ions by ethylamine modified chitosan carbonized rice husk composite beads with modeling and optimization, J. Chem.,2013 (2013) 11.
[4] G.N. Choppala, N. Bolan, J.H. Park, Chapter two: chromium contamination and its risk assessment in complex environmental settings, Adv. Agron., 120 (2013) 129–172.
[5] M.A. Shouman, N.A. Fathy, S.A. Khedr, A.A. Attia, Comparative biosorption studies of hexavalent chromium ion onto raw and modified palm branches, Adv. Phys. Chem., 2013 (2013) 1–9.
[6] S. Singh, B.N. Rai, L.C. Singh, Ni(II) and Cr(VI) sorption kinetics by microcystis in single and multimetallic system, Process Biochem., 36 (2001) 1205–1213.
[7] S. Hanif, A. Shahzad, Removal of chromuim(VI) and de Alizarin Red S (ARS) using polymer–coated iron oxide (Fe₃O₄) magnetic nanoparticles by co-precipitation method, J. Nanopart. Res., 16 (2014) 1–15.
[8] WHO, Guidelines for Drinking Water Quality, 4th ed., World Health Organization, Geneva, 2011.
[9] L. Alidokht, A.R. Khataee, A. Reyhanitabar, S. Oustan, Reductive removal of Cr(VI) by starch stabilized Fe⁰ nanoparticles in aqueous solution, Desalination, 270 (2011) 105–110.
[10] S.K. Natavaj, K.M. Hosamani, T.M. Aminabhavi, Distillery wastewater treatment by the membrane-based nanofiltration and reverse osmosis processes, Water Res., 40 (2006) 2349–2356.
[11] N.E. Davila-Guzman, F.J. Cerino-Cordova, M. Loredo-Ancino, J.R. Rangel-Mendez, R. Gomez-Gonzalez, E. Soto-Regalado, Studies of adsorption of heavy metals onto spent coffee ground: equilibrium, regeneration and dynamic performance in a fixed-bed column, Int. J. Chem. Eng., 2016 (2016) 1–11.
[12] N. Ilankoon, Use of iron oxide magnetic nanosorbents for Cr(VI) removal from aqueous solutions: a review, J. Eng. Res. Appl., 4 (2014) 55–63.
[13] M.A. Al-Anber, I.F. Al-Momani, Z.A. Al-Anber b, F. Almomani, The performance of defatted jojoba seeds for the removal of toxic high concentration of the aqueous ferric ion, Desal. Water Treat., 52 (2013) 1–12.
[14] J.A. Lakmono, M. Sudibandriyo, A.H. Saputra, A. Haryono, Development of Porous Structured Polyvinylalcohol/zeolite/ Carbon Composites as Adsorbent, 7th International Conference on Key Engineering Materials ICKEM, IOP Conf. Ser.: Mater. Sci. Eng., 201 (2017) 1–5.
[15] N.M. Mahmoodi, F. Najafi, S.Khorramfar, F.Amini, M.Arami, Synthesis, characterization and dye removal ability of high capacity polymeric adsorbent: polyaminoimide homopolymer, J. Hazard. Mater., 198 (2011) 87–94.
[16] T. Jamnonkan, K. Kantarot, K. Niemtang, P.P. Pansila, A. Waltanakornsiri, Kinetic and mechanism of adsorptive removal of copper from aqueous solution with poly(vinyl alcohol) hydrogel, Trans. Nonferrous Met. Soc. China, 24 (2014) 3386–3393.
[17] T.M. Budnyak, L.V. Pylypchuk, V.A. Tertykh, E.S. Yanoska, D. Kolodynska, Synthesis and adsorption properties of chitosan–silica nanocomposite prepared by sol-gel method, Nanoscale Res. Lett., 10 (2015) 87.
[18] Y.W. Mirzayanti, Experimental study on the use of chitosan-coated activated carbon to reduce the content of metal Fe the produced water, ARPN J. Eng. Appl. Sci., 10 (2015) 10506–10510.
[19] E. Salehi, A. Farahani, Macroporous chitosan polyvinyl alcohol composite adsorbents based on activated carbon substrate, J. Porous Mater., 24 (2017) 1197–1207.
[20] N. Azouaou, Z. Sadaoui, H. Mokaddem, Removal of lead from aqueous solution onto untreated coffee grounds: a fixed-bed column study, Chem. Eng. Trans., 38 (2014) 151–156.
[21] A.A. Attia, M.A. Shouman, S.A. Khedr, N.A. Hassan, Fixed-bed column studies for the removal of Congo red using *Simmondsia chinesis* (Jojoba) and coated with chitosan, Indonesian J. Chem., 18 (2018) 294–305.
[22] S. Bensadek, H. Aguedal, A. Iddou, A. Aziz, Biosorption of chromium(VI) in a fixed-bed column using adsorbent biomass, Key Eng. Mater., 800 (2019) 157–163.

[23] H. Panda, N. Tiadi, M. Mohanty, C.R. Mohanty, Studies on adsorption of an industrial waste for removal of chromium from aqueous solution, S. Afr. J. Chem. Eng., 23 (2017) 132–138.

[24] S. Yuksel, R. Orhan, The removal of Cr(VI) from aqueous solution by activated carbon prepared from apricot stone and almond shell mixture in a fixed-bed column, Arabian J. Sci. Eng., 23 (2018) 5345–5357.

[25] B. Sivaprakash, N. Rajamohan, A.M. Sadhik, Batch and column sorption of heavy metal aqueous solution using a marine algae *Sargassum tenerrimum*, Int. J. Chem. Tech. Res, 2 (2010) 155–162.

[26] H.D.S.S. Karunarathne, B.M.W.P Amarasinghe, Fixed-bed adsorption column studies for the removal of aqueous phenol from activated carbon prepared from sugarcane bagasse, Energy Procedia, 34 (2013) 83–90.

[27] Z.Z. Chowdhury, S.B. Abd Hamid, S. Zain, Evaluating design parameters for breakthrough curve analysis and kinetics of fixed-bed columns for Cu(II) cations using lignocellulosic wastes, Bioresources, 10 (2015) 732–749.

[28] C.P. Ling, I.A. Tan, L.L.P. Lim, Fixed-bed column study for adsorption of cadmium on oil palm shell-derived activated carbon, J. Appl. Sci. Process Eng., 3 (2016) 60–71.

[29] M.R. Majeed, Removal efficiency of heavy metals from aqueous solutions by albedo of pomelo fruit, Current Res. Microbiol. Biotechnol., 5 (2017) 1336–1344.

[30] P. Zheng, B. Bai, W. Guan, H. Wang, Y. Suo, Fixed-bed column studies for the removal of anionic dye from aqueous solution using TiO$_2$@glucose carbon composites and bed regeneration study, J. Mater. Sci.: Mater. Electron., 27 (2016) 867–877.

[31] U. Habiba, T.A. Siddique, T.C. Joo, A. Salleh, B.C. Ang, A.M. Afifi, Synthesis of chitosan/polyvinyl alcohol/zeolite composite for removal of methyl orange, Congo red and chromium(VI) by flocculation/adsorption, Carbohydr. Polym., 157 (2017) 1568–1576

[32] Y. Zhang, X. Huang, B. Duan, L. Wu, S.X. Yuan, Preparation of electrospun chitosan/poly(vinyl alcohol) membranes, Colloid Polym. Sci., 285 (2007) 855–863.

[33] A.A. Afifi, R.A. Youssef, M.M. Hussein, Fourier transform infrared spectrometry study on an early stage of salt stress in jojoba plant, Life Sci. J., 10 (2013) 1973–1981.

[34] B. Jeyagowri, R.T. Yamuna, Biosorption of Methylene blue from aqueous solutions by modified mesoporous *Simarouba glauca* seed shell powder, Global NEST J., 7 (2015) 701–7185.

[35] S. Hema, R. Ramya, P.N. Sudha. Preparation of chitin PVA/SF ternary blend for heavy metal ion removal from electroplating industrial effluent, Appl. Chem., 46 (2012) 8273–8278.

[36] M. Mirabedini, M.Z⎮. Kassaee, S. Poorsadeghi, Novel magnetic chitosan hydrogel film, cross-linked with glyoxal as an efficient adsorbent for removal of toxic Cr(VI) from water, Arabian J. Sci. Eng.,42 (2017) 115–124.

[37] F.F. Wang, M. Ge, Fibrous mat of chitosan polyvinyl alcohol/ containing cerium(III) for the removal of chromium(VI) from aqueous solution, Text. Res. J., 83 (2013) 628–637.

[38] D.K. Singh, V. Kumar, S. Mohin, D. Bano, S.H. Hasan, Breakthrough curve modeling of graphene oxide aerogel packed fixed-bed column for the removal of Cr(VI) from water, J. Water Process Eng., 18 (2017)150–158.

[39] S. Chowdhury, P.D. Saha, Artificial neural network (ANN) modeling of adsorption of Methylene blue by NaOH-modified rice husk in a fixed-bed column system, Environ. Sci. Pollut. Res., 20 (2013) 1050–1058.

[40] S. Srivastava, S.B. Agrawal, M.K. Mondal, Fixed-bed column adsorption of Cr(VI) from aqueous solution using nanoadsorbents derived from magnetite impregnated *Phaseolus vulgaris* husk, Environ. Prog. Sustainable Energy, 38 (2018) S68-S76.

[41] H.I. Albroomi, M.A. Elsayed, A. Baraka, M.A. Abdelmaged, Batch and fixed-bed adsorption of tartrazine azo-dye onto activated carbon prepared from apricot stones, Appl. Water Sci., 7 (2016) 2063–2074.

[42] H. Patel, R.T. Vashi, Fixed-bed column adsorption of acid yellow 17 dye onto tamarind seed powder, Can. J. Chem. Eng., 90 (2012) 180–185.

[43] R. Han, Y. Wang, X. Zhao, Y.F. Wang, F. Xie, J. Cheng, M. Tang, Adsorption of Methylene blue by phoenix tree leaf powder in a fixed-bed column: experiments and prediction of breakthrough curves, Desalination, 245 (2009) 284–297.

[44] R. Kaur, J. Singh, R. Khare, A. Ali, Biosorption the possible alternative to existing conventional technologies for sequestering heavy metal ions from aqueous streams: a review, Univ. J. Environ. Res. Technol., 2 (2012) 325–335.

[45] B. Singh, V. Thakur, G. Bhatia, D. Verma, K. Singh, Eco-friendly and cost-effective use of rice straw in the form of fixed-bed column to remove water pollutants, J. Biorem. Biodegrad., 7 (2016) 1–7.

[46] N. Vinodhini, N. Das, Packed bed column studies on Cr(IV) removal from tannery wastewater by neem sawdust, Desalination, 264 (2010) 9–14.